EUKARYOTIC CELL, May 2008, p. 906–916 Vol. 7, No. 5
1535-9778/08/$08.00+0 doi:10.1128/EC.00464-07


# Overlapping Functions of the Two Talin Homologues in *Dictyostelium*▽‡

Masatsune Tsujioka,[1,2]* Kunito Yoshida,[3]† Akira Nagasaki,[1] Shigenobu Yonemura,[2] Annette Müller-Taubenberger,[4] and Taro Q. P. Uyeda[1]

*National Institute of Advanced Industrial Science and Technology (AIST), Tsukuba Central 4, 1-1-1 Higashi, Tsukuba, Ibaraki 305-8562, Japan[1]; RIKEN, Center for Developmental Biology, 2-2-3 Minatojima-minamimachi, Chuo-ku, Kobe 650-0047, Japan[2]; Department of Botany, Graduate School of Science, Kyoto University, Sakyo-ku, Kyoto 606-8502, Japan[3]; and Institute for Cell Biology (ABI), Ludwig Maximilians University, Schillerstr. 42, 80336 Munich, Germany[4]*

Received 27 December 2007/Accepted 18 March 2008

**Talin is a cytoskeletal protein involved in constructing and regulating focal adhesions in animal cells. The cellular slime mold *Dictyostelium discoideum* has two talin homologues, *talA* and *talB*, and earlier studies have characterized the single knockout mutants. *talA*$^-$ cells show reduced adhesion to the substrates and slightly impaired cytokinesis leading to a high proportion of multinucleated cells in the vegetative stage, while the development is normal. In contrast, *talB*$^-$ cells are characterized by reduced motility in the developmental stage, and they are arrested at the tight-mound stage. Here, we created and analyzed a double mutant with a disruption of both *talA* and *talB*. Defects in adhesion to the substrates, cytokinesis, and development were more severe in cells with a disruption of both *talA* and *talB*. The *talA*$^-$ *talB*$^-$ cells failed to attach to the substrates in the vegetative stage, exhibited a higher proportion of multinucleated cells than *talA*$^-$ cells, and showed more-reduced motility during the development and an earlier developmental arrest than *talB*$^-$ cells at the loose-mound stage. Moreover, overexpression of either *talA* or *talB* compensated for the loss of the other talin, respectively. The analysis of *talA*$^-$ *talB*$^-$ cells also revealed that talin was required for the formation of paxillin-rich adhesion sites and that there was another adhesion mechanism which is independent of talin in the developmental stage. This is the first study demonstrating overlapping functions of two talin homologues, and our data further indicate the importance of talin.**

Formation and regulation of focal adhesions are crucial for cell locomotion, since cells need to adhere to substrates in order to exert traction forces. Talin is a large cytoskeletal protein which assembles at focal adhesions in mammalian cells (8). It is thought to link actin filaments to the plasma membrane at focal adhesions, since it has a FERM domain that interacts with the plasma membrane at the N terminus and an I/LWEQ module, which is an actin binding domain conserved in certain proteins, including talin and yeast Sla2, at the C terminus (22). This view is supported by the findings of previous studies that showed that inhibitions of talin's function or a disruption of a talin gene compromise the assembly and stabilization of focal adhesions (4, 27, 29). Several other studies have attempted to clarify not only the structural but also the regulatory role of talin. For instance, talin nucleates and organizes actin filaments and is involved in the processing and activation of integrins (1, 13, 34). Talin binds and regulates type Iγ phosphatidylinositol phosphate kinase at synapses and focal adhesions (9, 19, 21, 24). Furthermore, talin is implicated in cytokinesis through a so-far-unknown mechanism (3, 14, 26).

It is intriguing that a second talin has been discovered for certain organisms, considering the wide spectrum of functions of talin (30). The cellular slime mold *Dictyostelium discoideum* was the first organism for which two different talin homologues, talin A and talin B, which are encoded by *talA* and *talB*, respectively, have been identified. *Dictyostelium* is an established model system to study the mechanisms of cell movement. It possesses a large number of cytoskeletal proteins that are also present in mammalian cells, and the amoeboid cells move actively, in a manner similar to that of leukocytes (11). The availability of various genetic approaches allowed for identifying genes involved in diverse processes and revealing the dynamics and functions of the gene products. When deprived of a food supply, the amoeboid cells aggregate and build up a hemispherical structure called a "mound." A small protrusion forming a "tip" subsequently emerges from the top of the mound, which then can elongate to form a cylindrical structure known as a "slug" that finally transforms into a fruiting body consisting of a stalk tube and a spore sorus.

There are clear phenotypic differences between *talA*$^-$ and *talB*$^-$ strains that appear to suggest distinct roles for the two talins. Talin A's main role appears to be in the vegetative stage. *talA*$^-$ cells show much weaker adhesion to the substrates and bacterial surfaces than wild-type cells, resulting in a distinct phagocytosis defect, and improper cytokinesis, resulting in multinucleated cells in suspension cultures during the vegetative stage. Although severe defects are observed during the growth phase, development in *talA*$^-$ cells proceeds normally (26). In contrast to *talA*$^-$ cells, cells lacking talin B are defective in development, although the cells do not exhibit any obvious deficiencies during the vegetative stage (35). *talB*$^-$

* Corresponding author. Mailing address: RIKEN, Center for Developmental Biology, 2-2-3 Minatojima-minamimachi, Chuo-ku, Kobe 650-0047, Japan. Phone: 81-78-306-3106. Fax: 81-78-306-3107. E-mail: mas-tsujioka@cdb.riken.jp.

† Present address: MRC Laboratory of Molecular Biology, Hills Road, Cambridge CB2 0QH, United Kingdom.

‡ Supplemental material for this article may be found at http://ec.asm.org/.

▽ Published ahead of print on 28 March 2008.

cells never form a tip on the mound, probably due to weaker motile forces of the differentiated cells within the mounds (36).

Recent studies suggested that the two mammalian talins also have discernible functions. Talin 1 was suggested to have a function in myoblasts, while talin 2 is induced during striated muscle differentiation. In addition, talin 1 and talin 2 mRNAs show different distributions in adult mouse tissues (31). Different binding partners have been described for mouse talin 1 and talin 2 (30). Disruption of the *tln1* gene encoding talin 1 in mice leads to embryonic death due to an incomplete gastrulation, indicating that talin 2, encoded by *tln2*, is not able to compensate for the loss of talin 1 (23). Similarly, talin 2 is not able to replace talin 1 in the formation of the minimal linkage between fibronectin and the cytoskeleton in mouse differentiated embryonic stem cells (16), although the expression of *tln2* was not examined in these two experiments. Furthermore, alternative variants of a talin gene in the nonvertebrate chordate *Ciona intestinalis* are suggested to have different roles (32). However, the analysis of a double mutant with a disruption of both talin genes and the rescue of a mutant lacking one talin gene by the overexpression of the other talin gene, which would enable us to clearly demonstrate the unique and overlapping functions of two talins, have never been attempted. Here, we applied our analysis to the two talins in *Dictyostelium discoideum* and provided evidence that the functions of the two talins were largely redundant. The more-severe phenotypic defects of the double mutant further confirm the important role of talin.

## MATERIALS AND METHODS

**Cloning of expression constructs.** To create the green fluorescent protein (GFP)-paxillin construct, full-length *paxB* paxillin cDNA (5) was amplified from a *Dictyostlium* cDNA library by PCR using the primer set 5′-GGATCCAATG TCAAATAAAAATCCATTAAATAATAGTA-3′ and 5′-GAGCTCTTATTTT CTTTGTTGTACAAGTGT-3′. The PCR product was fused to GFP cDNA by subcloning into GFP/pBIG vector (25) as a BamHI/SacI fragment.

To generate the FLAG-tagged full-length talin B construct, three parts of *talB* cDNA (4 to 1164, 2988 to 7275, and 6234 to 7845, numbered from the first nucleotide of the coding sequence) were obtained from a *Dictyostlium* cDNA library by PCR or from total RNA by reverse transcription (RT)-PCR using three primer sets: 5′-CGAGCTCTCACTTACACTCAAGATTCAAATCGT-3′ and 5′-GGAATTCACTCTCAACGTTGGCAATATCAG-3′, 5′-CGTTCAAG CCTTAGAAGCCG-3′ and 5′-GATGATTTGGGCGTTTGATAAG-3′, and 5′-GGCTGCTTATGATAGTGCAACC-3′ and 5′-GCTCTAGATTAGAATAAA CCAAGTTTAGTTTTTATATTATTTC-3′, respectively. The fragment 4 to 1164 was subcloned into the pCRBluntIITOPO vector as a SacI/EcoRI fragment (ptalB-head). A KpnI/KpnI fragment of the *talB* gene was acquired from the plasmid containing the *talB* knockout construct, which was obtained using XbaI from the genome of the *talB*$^-$ mutant (35). The fragment was inserted into ptalB-head that was digested with KpnI to extend the *talB* cDNA fragment (ptalB-Nhalf). The fragment 6234 to 7845 was subcloned into HincII/XbaI-digested pBluescriptIISK+ after digestion with the same enzymes (ptalB-tail). A KpnI/EcoRI fragment of ptalB-tail was replaced by a KpnI/EcoRI fragment of the fragment 2988 to 7275 to obtain a longer *talB* cDNA fragment (ptalB-Chalf). A SacI/SacI fragment and a SacI/XbaI fragment from ptalB-Nhalf and ptalB-Chalf, respectively, were ligated to the SacI/XbaI-digested pTX-FLAG (20) construct to complete the expression construct of FLAG-tagged full-length talin B.

To create the talin A-GFP construct, which drives the expression of talin A fused with GFP at the C terminus, the full-length *talA* gene was amplified by PCR using the primer set 5′-GATCGGATCCAATGTCAATTTCATTAAAAA TTAATATTGTTGG-3′ and 5′-ATCGGATCCATTTTTATTATAATTTTGTT TTCTTG-3′. The PCR product was subcloned into pA15GFP vector (kindly provided by Rex Chisholm, Northwestern University) as a BamHI/BamHI fragment.

**Strains and conditions for growth and development.** Strains used in the present study were *Dictyostelium* Ax2 as a wild-type strain, HG1664 as a *talA*$^-$ strain (26), HKT104 as a *talB*$^-$ strain (36), and a strain with a disruption of both *talA* and *talB* (a *talA*$^-$ *talB*$^-$ strain). All the strains were grown axenically in HL5 axenic medium (0.5% yeast extract, 0.5% peptone, 1% glucose, 8.82 mM $KH_2PO_4$, 2.46 mM $Na_2HPO_4$ [pH 6.3]) at 22°C in plastic petri dishes (33). FLAG-tagged talin B and talin A-GFP constructs were introduced separately into *talA*$^-$, *talB*$^-$, and *talA*$^-$ *talB*$^-$ strains. GFP-actin and GFP-paxillin constructs were introduced into wild-type and *talA*$^-$ *talB*$^-$ strains separately. The expression of all the tagged proteins was driven by actin 15 promoter. Those transformants were selected in HL5 axenic medium containing 10 μg/ml G418. Cells were allowed to develop at 22°C on 1% nonnutrient agar buffered with $KK_2$ phosphate (16.5 mM $KH_2PO_4$ and 3.8 mM $K_2HPO_4$, pH 6.2) or on a lawn of *Klebsiella aerogenes* made on SM/5 agar plates (33).

**Analysis of translational regulations.** Wild-type cells growing exponentially in HL5 shaken cultures ($2 \times 10^6$ to $5 \times 10^6$ cells/ml) were harvested and washed once in $KK_2$ phosphate buffer. The cells were resuspended in $KK_2$ phosphate buffer at a density of $5 \times 10^4$ cells/μl, and the cell suspension was spotted as 10-μl aliquots on mixed cellulose ester filters (Advantec). The membrane filters were placed on filter papers (Advantec) soaked with $KK_2$ phosphate buffer and were kept at 22°C to allow cells to develop. Cells ($10^7$) were taken every 3 h after the onset of development to be lysed in 100 μl of sample buffer (75 mM Tris-HCl [pH 6.8], 3% sodium dodecyl sulfate [SDS], 9% β-mercaptoethanol, 15% glycerol, and 0.075% bromophenol blue). For Western blotting analysis, 15 μl of the lysates was fractionated by SDS-polyacrylamide gel electrophoresis (PAGE) (SuperSep 5 to 20%; WAKO) and transferred to polyvinylidene difluoride membranes. Talin A and talin B were visualized by chemiluminescence assay (Immobilon Western; Millipore) using their specific antibodies as in previous studies (18, 36) and horseradish peroxidase-conjugated anti-rabbit or anti-mouse secondary antibody (Jackson ImmunoResearch). To confirm the equal loading amounts, 3 μl of lysates was subjected to SDS-PAGE, and the gel was stained with Coomassie blue.

**Analysis of gene expression by RT-PCR.** *talB*$^-$ and *talA*$^-$ *talB*$^-$ cells were allowed to develop on membrane filters as described for sample preparation for Western blotting analysis. After 36 h, total RNA was extracted from the mounds by using an RNeasy Mini kit (Qiagen). RT-PCR was performed using total RNA, a Titanium one-step RT-PCR kit (BD Biosciences), and specific primer sets to amplify the genes.

**Generation of a *talA*$^-$ *talB*$^-$ double mutant.** For the generation of a *talA*$^-$ *talB*$^-$ double mutant, $8 \times 10^6$ blasticidin-resistant *talA*$^-$ cells were transformed by electroporation with the disruption construct of *talB* carrying a hygromycin resistance cassette (36). The resultant cells were diluted in HL5 axenic medium containing 10 μg/ml blasticidin S (Funakoshi, Japan) and 50 μg/ml hygromycin B (Wako), and the aliquots were seeded into six 96-well plates. In addition, autoclaved bacteria were included in the selection medium to raise the efficiency of transformation (17). For the preparation of autoclaved bacteria, *K. aerogenes* grown in YT medium (2% tryptone, 1% yeast extract, 1% NaCl) at 37°C overnight were collected, washed twice with $KK_2$ phosphate buffer, and concentrated 100× in $KK_2$ phosphate buffer. The bacteria slurry was autoclaved and added to HL5 axenic medium at a 100-fold dilution. Cells that were resistant to both blasticidin S and hygromycin B appeared in a small number of wells after the selection, and those clones were transferred to a plate with a lawn of *K. aerogenes* to observe the morphogenesis during development. Disruption of the *talB* gene by homologous recombination was confirmed by genomic PCR using primers 5′-CGAAACACACAACAACAAAATACAC-3′ and 5′-GACCACCTTTAAC AATTTCAATTGCC-3′.

**Adhesion assays.** For the adhesion assay, $10^6$ cells in 1 ml HL5 axenic medium were plated into plastic petri dishes (35-mm nontreated dish; Iwaki). Cells were allowed to settle and adhere to the bottom surfaces for 20 min, and then the dishes were agitated by using an orbital shaker at speeds ranging from 0 to 200 rpm for 30 min. Subsequently, the media containing detached cells were taken, and the fractions of detached cells were determined by counting.

For the adhesion assay in $KK_2$ phosphate buffer, $10^6$ cells grown in HL5 axenic medium were collected by using a microcentrifuge (MX-300; Tomy) at 10,000 rpm for 5 seconds and were suspended in 1 ml $KK_2$ phosphate buffer or HL5 axenic medium for a control. The cell suspension was immediately transferred into 35-mm nontreated dishes. The fraction of nonadherent cells was determined by counting the cells contained in the supernatant removed from the dishes after 5 min. To assay the inhibition of adhesion in HL5 axenic medium, $10^6$ *talA*$^-$ *talB*$^-$ cells grown axenically were allowed to adhere to the bottom surfaces of 35-mm nontreated dishes in 1 ml $KK_2$ phosphate buffer for 20 min. After the fraction of adherent cells was determined by counting the nonadherent cells in the buffer removed from the dishes, the adherent cells were incubated in 1 ml

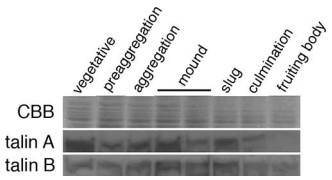


FIG. 1. Time courses of talin A and talin B expression. Wild-type cells developing on membrane filters were harvested every 3 h and were lysed in SDS sample buffer. Equal amounts of lysates were separated by three individual SDS-PAGEs. One was used for the staining with Coomassie blue (CBB) to confirm the equal amount of loading, and the other two were used for Western blotting analysis to examine the time courses of talin A and talin B expression, which was detected using each specific antibody. Only a portion of the gel is shown for Coomassie blue staining (top).

HL5 axenic medium for 3 h. The fraction of detached cells was subsequently determined by counting the number of cells contained in the removed medium. The control experiment was performed by the same procedure except with $KK_2$ phosphate buffer for the 3-h incubation instead of HL5 axenic medium.

To assay adhesion to the agar surface, 1 ml of a cell suspension grown in HL5 axenic medium to a density of $10^6$ cells/ml was placed on a 0.5% nonnutrient agar plate. After 30 min, the medium containing nonadherent cells was removed by slanting the dish to determine the proportion of nonadherent cells.

**Recording cell movement and fluorescence microscopy.** Vegetative cells were harvested and resuspended in $KK_2$ phosphate buffer. An aliquot of the cell suspension was placed in a glass-bottom dish (35-mm; Iwaki) and overlaid with a thin piece of a sheet made of 1% nonnutrient agar. The agar sheet was produced by pouring 3 ml of melted agar of $KK_2$ phosphate buffer into a 6-cm plastic dish (Falcon). After 4 h, phase-contrast images of the cells were captured every 3 min for 90 min using NIH Image software version 1.62 and an inverted microscope (IX50; Olympus, Japan) equipped with a charge-coupled-device camera (C5985; Hamamatsu Photonics, Japan) and a time-lapse system (Argus-20; Hamamatsu Photonics). The cell centroids were tracked using ImageJ software version 1.32, and the mean velocity of cell migration was determined by averaging the displacements during 3-min intervals. Fluorescent signals of GFP-actin and GFP-paxillin in the transformants were observed using a confocal microscope (CSU10; Yokogawa, Japan).

**Analysis of development.** Vegetative cells ($2 \times 10^6$) were collected by centrifugation at 2,000 rpm for 3 min and suspended in 100 μl $KK_2$ phosphate buffer. Aliquots (10 μl) of the cell suspensions were spotted on 1% nonnutrient agar to allow the cells to develop. Pictures of the spots were taken at certain time points by using a stereo microscope (MZ7.5; Leica) equipped with a charge-coupled-device camera (FX380; Olympus) to monitor the developmental processes. Different spots were photographed at the onset and after 12 h of development.

**Cytokinesis assay.** Cells ($3 \times 10^5$) were grown axenically on 0.5% nonnutrient agar submerged in 3 ml HL5 axenic medium in 6-cm plastic petri dishes to a cell density of approximately $2 \times 10^6$ cells/ml, and nonadherent cells were collected by centrifugation. The harvested cells were fixed with 1% formaldehyde in ethanol at −20°C. After the cells were washed three times with phosphate-buffered saline (PBS; 137 mM NaCl, 2.68 mM KCl, 8.1 mM $Na_2HPO_4$, 1.47 mM $KH_2PO_4$), they were incubated in PBS containing 1 μg/ml DAPI (4′,6′-diamidino-2-phenylindole) for 10 min. Subsequently, cells were washed three times with PBS, and the number of nuclei was counted using an IX70 fluorescence microscope.

## RESULTS

**Developmental time courses of talin A and talin B expressions.** The defects of *talA*$^-$ and *talB*$^-$ cells are seen only in the vegetative and developmental stages, respectively. We first analyzed the translational regulations of talin A and talin B during development by Western blotting analysis in order to examine whether they are expressed mainly in the stages where each mutant exhibits the impairments. Both proteins were present in the vegetative stage and throughout development, although the patterns were different for the two stages. Talin A was maximally expressed in the vegetative stage, and considerable accumulations occurred at the mound and slug stages (Fig. 1). In contrast, the expression of talin B reached the maximum between mound and slug stages (Fig. 1). Therefore, each talin exhibited plausible maximal accumulations at times when it was suggested to play a more important role based on the mutant analysis, but considerable levels of expression were also detected in other periods for both talins.

**Generation of a *talA*$^-$ *talB*$^-$ double mutant.** In order to obtain a *Dictyostelium* double mutant lacking both talin A and talin B, we eliminated talin B in *talA*$^-$ cells (26). *talA*$^-$ cells were transformed with a disruption construct targeted against *talB* (Fig. 2A) (36). Transformed cells, which were potential candidates of *talA*$^-$ *talB*$^-$ double-mutant clones, emerged following selection. We transferred the transformant clones to bacterial lawns to observe their developmental phenotype. Only 12 out of 142 clones from two independent transformations were arrested at the mound stage, and the remainder formed normal fruiting bodies. Since the inactivation of *talB* in wild-type cells resulted in a developmental arrest at the tight-mound stage (35), we selected 4 of the 12 clones that were arrested at the mound stage and tested them for disruption of *talB*. Genomic PCR analysis confirmed that the *talB* genes of all four clones were replaced by the knockout construct due to homologous recombination (Fig. 2B). In contrast, *talB* genes in two resistant clones that formed fruiting bodies were not disrupted, suggesting that the constructs were integrated into the genome nonhomologously (Fig. 2B).

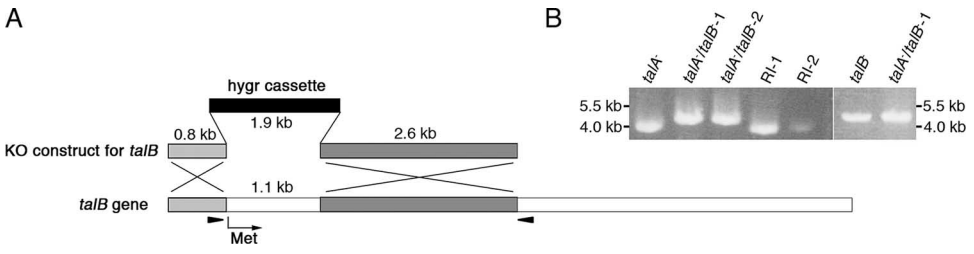


FIG. 2. Disruption of the *talB* gene in *talA*$^-$ cells. (A) Schematic representation of the *talB* gene disruption with the disruption construct (36). The sites of the first codon of *talB* and the positions of the primers used to confirm the disruption are indicated by an arrow and arrowheads, respectively. (B) Confirmation of *talB* gene disruption by PCR using genomic DNA as the template. The bands obtained with the indicated primers (arrowheads in panel A) were approximately 4 kb in size in the parent *talA*$^-$ strain and also in the two clones of random integrants (RI-1 and 2) whose *talB* genes were not disrupted. In contrast, the bands obtained from genomic DNA of the *talB*$^-$ strain and the two clones of the *talA*$^-$ *talB*$^-$ strain were 0.8 kb larger in size due to the replacement of a 1.1-kb fragment of *talB* gene by the 1.9-kb hygromycin cassette.

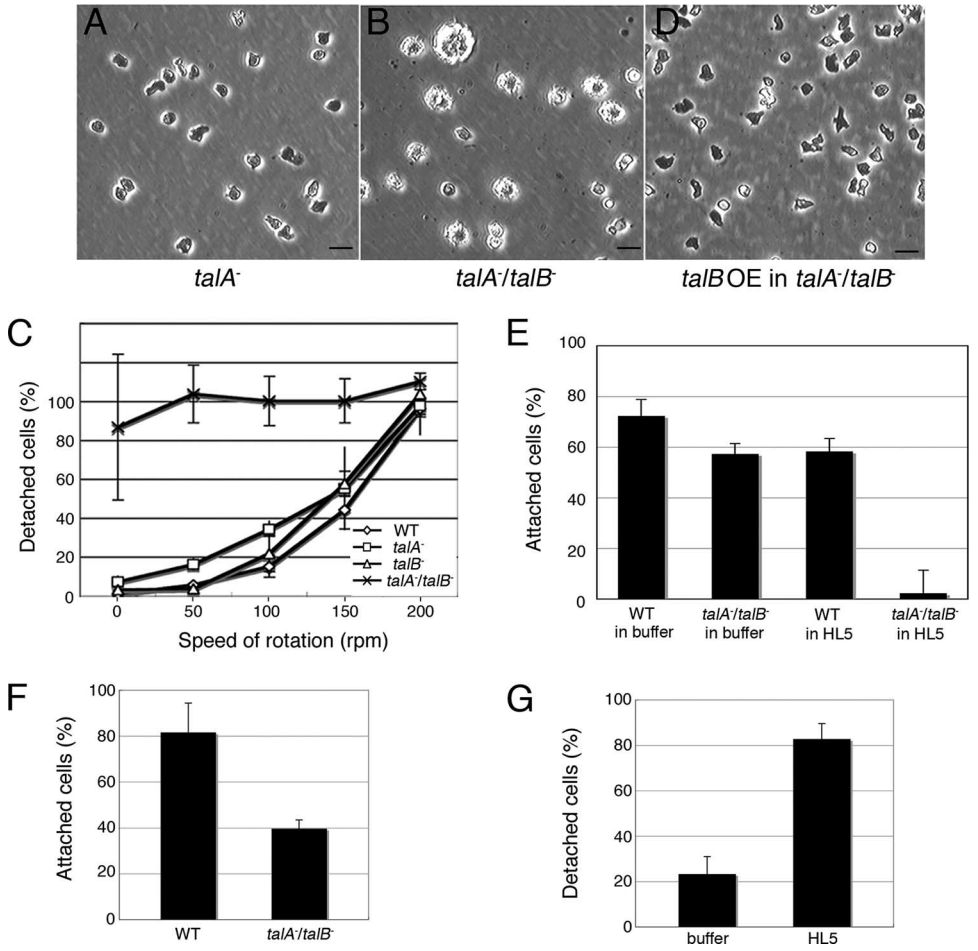


FIG. 3. Attachment of wild-type (WT) and talin mutant cells to a solid substrate. (A, B, and D) Phase-contrast micrographs of *talA*$^-$ (A), *talA*$^-$ *talB*$^-$ (B), and *talA*$^-$ *talB*$^-$ cells expressing FLAG-tagged talin B (*talB* OE in *talA*$^-$/*talB*$^-$) (D) grown in HL5 axenic medium in plastic petri dishes. *talA*$^-$ *talB*$^-$ cells are more spherical and enlarged than *talA*$^-$ and *talB* OE in *talA*$^-$ *talB*$^-$ cells. The scale bars represent 20 μm. (C) Fractions of detached cells in HL5 axenic medium examined after 30 min of shaking the dishes. (E) Fractions of adherent cells examined 5 min after substituting $KK_2$ phosphate buffer for HL5 axenic medium or maintained in HL5 axenic medium. (F) Fractions of cells that remained attached in $KK_2$ phosphate buffer after 30 min of shaking the dishes at a speed of 75 rpm. (G) Fractions of detached *talA*$^-$ *talB*$^-$ cells, which had been induced to adhere to the substrates in $KK_2$ phosphate buffer, after the incubation in HL5 axenic medium or $KK_2$ phosphate buffer for 3 h. All data are means ± standard deviations (SD; $n = 3$).

***talA*$^-$ *talB*$^-$ double-mutant cells are severely affected in adhesion to substrates.** Phenotypic differences in comparison to control strains became obvious when *talA*$^-$ *talB*$^-$ cells were grown axenically in plastic petri dishes. Unlike wild-type and both *talA*$^-$ and *talB*$^-$ cells, most of the *talA*$^-$ *talB*$^-$ cells were spherical in shape and unable to attach to the substrates. Furthermore, many of the *talA*$^-$ *talB*$^-$ cells were significantly larger than wild-type and both *talA*$^-$ and *talB*$^-$ cells (Fig. 3A and B and data not shown).

In order to investigate wild-type, *talA*$^-$ and *talB*$^-$ single-mutant, and *talA*$^-$ *talB* $^-$ double-mutant cell adhesion to the surfaces of plastic petri dishes, we counted the number of detached cells after shaking the dishes at different speeds for 30 min. More than 60% of wild-type and both *talA*$^-$ and *talB*$^-$ cells remained attached at 100 rpm, whereas *talA*$^-$ *talB*$^-$ cells, even without shaking, were nonadherent (Fig. 3C). This result indicates that both talin A and talin B are involved in adhesion to the substrates in the vegetative stage and that expression of either talin gene is sufficient for an adhesion strength comparable to that of wild-type cells in this assay. The number of nonattached *talA*$^-$ *talB*$^-$ cells was smaller in the absence than in the presence of shaking. This was not a consequence of a few cells being able to adhere in the absence of shaking but instead occurred because it was difficult to remove all detached cells from the bottoms of the dishes under these conditions. Expression of FLAG-tagged talin B in *talA*$^-$ *talB*$^-$ cells restored their ability to adhere to the surfaces of plastic dishes (Fig. 3D). This result confirms that the defect in attachment to the substrates is due to the *talA*$^-$ *talB*$^-$ double mutation.

The *talA*$^-$ *talB*$^-$ mutant formed mounds, which suggests that *talA*$^-$ *talB*$^-$ cells are able to attach to the substrates for translocation after starvation. Therefore, we examined adhesion of *talA*$^-$ *talB*$^-$ cells to the substrates in the absence of nutrient medium. We collected both wild-type and *talA*$^-$ *talB*$^-$ cells from HL5 axenic medium, suspended the cells in $KK_2$ phosphate buffer at the same cell density, and plated the cell

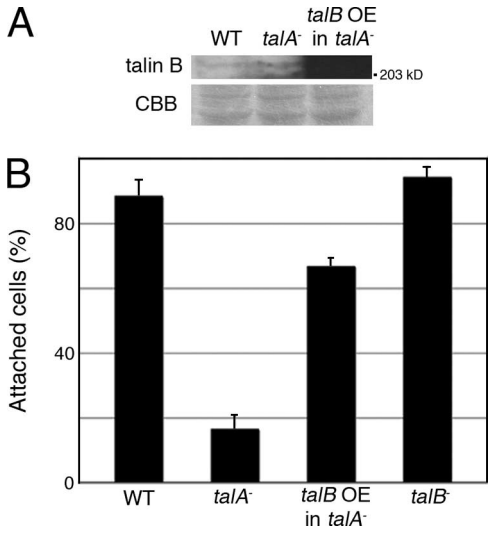


FIG. 4. Overexpression of FLAG-tagged talin B rescued the adhesion defect in the *talA*$^-$ mutant. (A) Vegetative wild-type (WT) cells, *talA*$^-$ mutant cells, and the transformant expressing FLAG-tagged talin B (*talB* OE in *talA*$^-$) were lysed in SDS sample buffer. Equal amounts of lysates were separated by two individual SDS-PAGEs. One was used for the staining with Coomassie blue (CBB) to confirm the equal loading amounts, and the other was used to examine the expression of internal talin B or FLAG-tagged talin B by Western blotting analysis using anti-talin B antibody. The signal in the transformant was so strong that it did not appear as a band with this exposure time. Only a portion of the gel is shown for staining of Coomassie blue. (B) Fractions of cells adherent to agar surfaces under submerged conditions in HL5 axenic medium after 30 min of settling. All data are means ± SD ($n$ = 3).

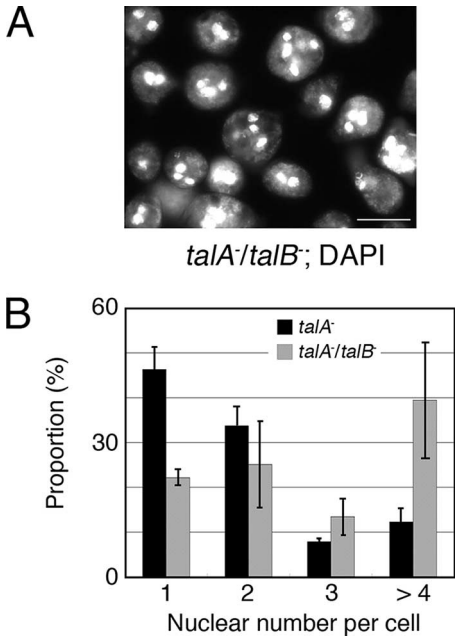


FIG. 5. Cytokinesis defect of *talA*$^-$ *talB*$^-$ cells. (A) Fluorescence images of DAPI-stained *talA*$^-$ *talB*$^-$ cells grown in HL5 axenic medium in a petri dish. (B) Comparison of the number of nuclei per cell between *talA*$^-$ and *talA*$^-$ *talB*$^-$ cells cultivated under detached and static conditions. All data are means ± SD ($n$ = 3).

suspensions immediately in plastic petri dishes. Nonadherent cells were counted after 5 min. Approximately 57% of *talA*$^-$ *talB*$^-$ cells were able to attach to the substrate under these conditions, although a higher fraction (72%) of wild-type cells adhered to the surfaces (Fig. 3E). When we used HL5 axenic medium instead of $KK_2$ phosphate buffer as a control in this assay, almost no cells attached to the bottom surfaces of the dishes (Fig. 3E). The weak adhesion ability of *talA*$^-$ *talB*$^-$ cells compared to wild-type cells in $KK_2$ phosphate buffer became more obvious when the shaking adhesion assay was carried out with $KK_2$ phosphate buffer (Fig. 3F). Only 40% of *talA*$^-$ *talB*$^-$ cells remained attached to the substrates after shaking, in contrast to 82% of wild-type cells. These results demonstrate that, unlike results with the nutrient medium, *talA*$^-$ *talB*$^-$ cells are able to adhere to the substrates in the nonnutrient $KK_2$ buffer, although more weakly than wild-type cells.

Subsequently, we examined whether the addition of HL5 axenic medium inhibited the attachment of *talA*$^-$ *talB*$^-$ cells that became adherent to the substrates in $KK_2$ phosphate buffer. *talA*$^-$ *talB*$^-$ cells, which had been allowed to attach to the substrates in $KK_2$ phosphate buffer in advance, were incubated in HL5 axenic medium for 3 h, and the fraction of detached cells was determined. Approximately 80% of *talA*$^-$ *talB*$^-$ cells detached in this assay, while only 20% of them detached when they were incubated in $KK_2$ phosphate buffer for 3 h instead of in HL5 axenic medium (Fig. 3G). The inactivation of adhesion ability by HL5 axenic medium was not as fast as the activation of adhesion by $KK_2$ phosphate buffer, since most of the *talA*$^-$ *talB*$^-$ cells remained attached 5 min after the buffer was replaced by HL5 axenic medium.

**Overexpression of FLAG-tagged talin B compensates for the adhesion defect in the *talA*$^-$ mutant.** We were unable to find any significant differences in the adhesion levels between wild-type and *talA*$^-$ cells in our assay described above (Fig. 3C), even though *talA*$^-$ cells have been reported to be impaired in adhesion to the substrates during the vegetative stage (26). Therefore, another, more sensitive assay was developed in order to compare adhesiveness between wild-type and *talA*$^-$ cells. When *talA*$^-$ cells were allowed to adhere to the surfaces of agar submerged in HL5 axenic medium, approximately 80% of *talA*$^-$ cells did not attach to the agar surfaces after 30 min of settling. In contrast, almost all wild-type and *talB*$^-$ cells attached, demonstrating the weaker adhesion ability of *talA*$^-$ cells (Fig. 4B). However, overexpression of FLAG-tagged talin B in *talA*$^-$ cells raised the fraction of attached cells by 67% (Fig. 4A and B).

**Cytokinesis of *talA*$^-$ *talB*$^-$ cells.** Since a considerable proportion of *talA*$^-$ *talB*$^-$ cells grown submerged in HL5 axenic medium in plastic petri dishes were significantly larger than wild-type cells, we stained the nuclei of these cells with DAPI and found that the enlarged cells were multinucleated (Fig. 5A). The deficiency of talin A causes impairment in substrate-independent cytokinesis, which is consistent with the multinucleation of *talA*$^-$ *talB*$^-$ cells, although *talA*$^-$ cells are able to divide almost normally when they adhere to the substrates (26). In order to compare the numbers of nuclei in *talA*$^-$ and *talA*$^-$ *talB*$^-$ cells grown in plastic petri dishes with HL5 axenic medium under static detached conditions, we incubated both strains on nonnutrient agar submerged in HL5 axenic medium, which significantly inhibited the substrate ad-

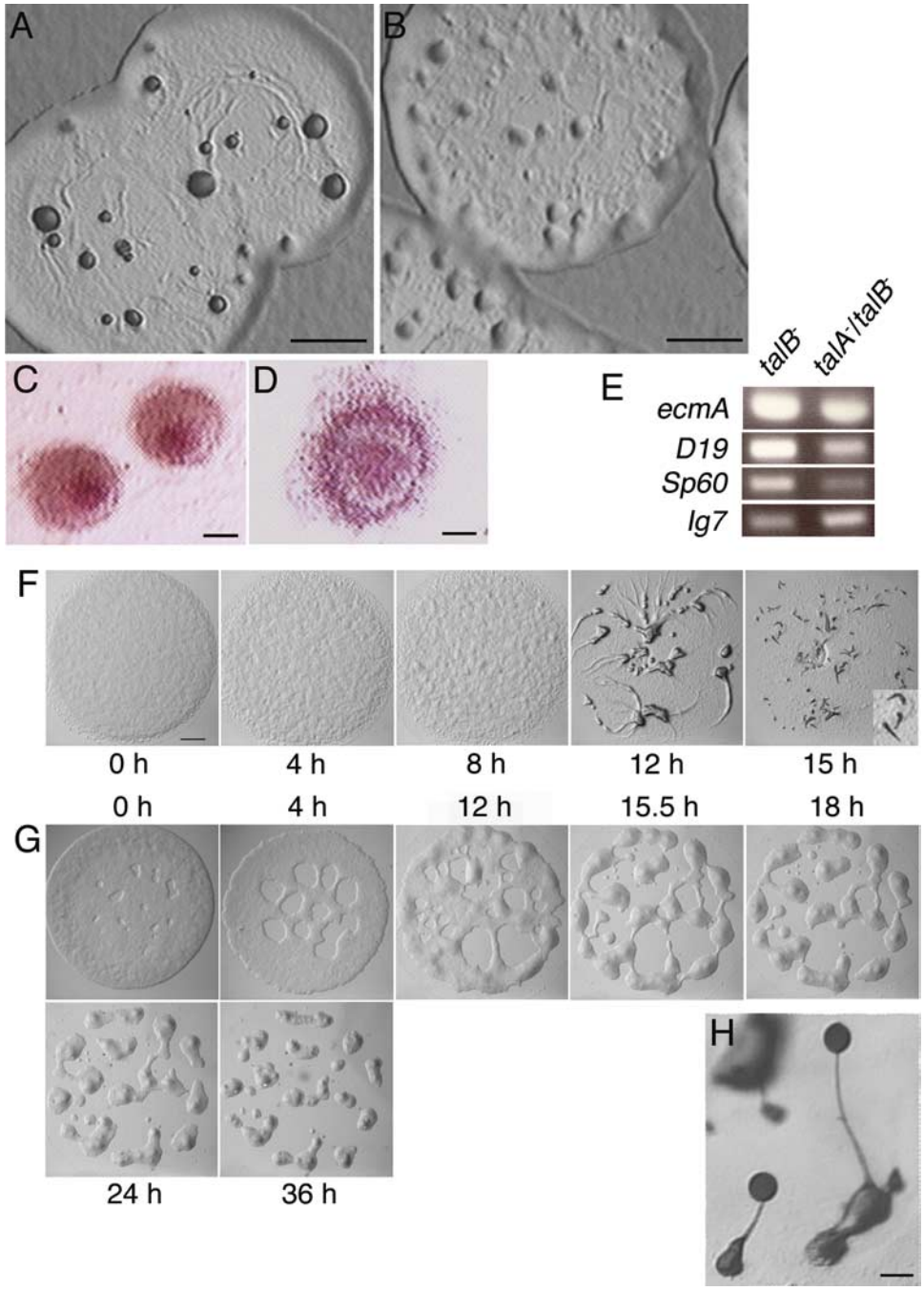


FIG. 6. Development in the *talA*$^-$ *talB*$^-$ double mutant is arrested at an earlier stage than in the *talB*$^-$ single mutant. (A and B) Top views of the plaques on bacterial lawns of *talB*$^-$ (A) and *talA*$^-$ *talB*$^-$ (B) strains. Cells inside the edges of the plaques started morphogenesis due to starvation. (C and D) The mounds of *talB*$^-$ (C) and *talA*$^-$ *talB*$^-$ (D) mutants stained with neutral red. (E) RT-PCR analysis of the marker genes in the development of *talB*$^-$ and *talA*$^-$ *talB*$^-$ mutants. The expression levels of a prestalk-specific gene, *ecmA*, and two prespore-specific genes, *SP60* and *D19*, were analyzed at the mound stage in *talB*$^-$ and *talA*$^-$ *talB*$^-$ mutants by RT-PCR using primer sets to amplify each gene fragment. *Ig7* is a constitutively expressed gene used as the control. (F and G) The processes of mound formation in wild-type (F) and *talA*$^-$ *talB*$^-$ (G) strains. Slugs formed at 15 h in wild-type cells are magnified in the bottom right corner of panel F. (H) Fruiting bodies formed by *talA*$^-$ *talB*$^-$ cells expressing FLAG-tagged talin B. The scale bars represent 1 mm (A, B, and F), 100 μm (C and D), and 20 μm (H).

hesion of *talA*$^-$ cells as described above, and we counted the number of nuclei of the detached cells. *talA*$^-$ cells seemed to exhibit significant multinucleation, as expected, though we were not able to compare it with that of wild-type cells, because almost all wild-type cells adhered to the agar surface in this assay. More importantly, *talA*$^-$ *talB*$^-$ cells showed more-severe impairment in cytokinesis than *talA*$^-$ cells under these conditions (Fig. 5B).

***The talA*$^-$ *talB*$^-$ double mutant is arrested at the early mound stage.** The *talB*$^-$ mutant is arrested at the tight-mound

stage, when the two cell types, prestalk cells and prespore cells, have already differentiated and their mutual sorting has occurred within the mound (35). We observed that the mound of *talA*$^-$ *talB*$^-$ mutant was flatter and more loosely packed than that of the *talB*$^-$ mutant (Fig. 6A and B). The flat and loose hemispherical structure is generally called a "loose mound" and occurs following completion of cell aggregation before cell sorting occurs within the mound. When allowed to develop on nonnutrient agar containing neutral red, which specifically stains prestalk cells, the red staining clearly concentrated at the top of the mound in the *talB*$^-$ mutant, as reported previously (Fig. 6C) (35). However, stained cells remained at the periphery of the mound and did not noticeably accumulate at the top of the mound in the *talA*$^-$ *talB*$^-$ mutant, suggesting that cell sorting has not been completed yet (Fig. 6D). In order to confirm the earlier developmental block of the *talA*$^-$ *talB*$^-$ mutant, we compared the expression levels of a prestalk-specific gene, *ecmA*, and prespore-specific genes *SP60* and *D19*, the expression of all of which increases during tight-mound formation, between the mounds formed by the *talB*$^-$ and *talA*$^-$ *talB*$^-$ mutants (10, 15, 28). RT-PCR analysis demonstrated that all the three genes were less expressed in the mounds of the *talA*$^-$ *talB*$^-$ mutant than in the *talB*$^-$ mounds (Fig. 6E). Therefore, not only cell sorting but also differentiation was impaired in the mounds of the *talA*$^-$ *talB*$^-$ mutant, further implying that there is an earlier developmental arrest for the *talA*$^-$ *talB*$^-$ mutant.

We also monitored carefully the processes of mound formation of wild-type and *talA*$^-$ *talB*$^-$ cells on nonnutrient agar by taking pictures at certain time points. In wild-type cells, aggregation domains became visible on lawns of cells at about 8 h; these domains resulted in the rough surfaces of the lawns, and streams of cells were clearly visible at about 12 h when elongated cells were moving toward the aggregation centers to form mounds. Many of the wild-type mounds formed slugs at 15 h (Fig. 6F). In contrast, the lawns of *talA*$^-$ *talB*$^-$ cells gradually separated into mounds without forming discernible streams, and the formation of the loose-mound structures was completed at approximately 36 h (Fig. 6G).

Expression of FLAG-tagged talin B in *talA*$^-$ *talB*$^-$ cells rescued the developmental defect, confirming that disruption of *talB* caused the developmental phenotype of the *talA*$^-$ *talB*$^-$ double mutant (Fig. 6H).

**Overexpression of talin A-GFP rescued the developmental block of the *talB*$^-$ mutant.** The fact that developmental arrest of the *talA*$^-$ *talB*$^-$ mutant occurred earlier than that of the *talB*$^-$ mutant suggests that talin A is also involved in the developmental process. Therefore, we transformed *talB*$^-$ cells with the talin A-GFP expression construct, which was able to rescue the defects of adhesion to bacterial surfaces and of cytokinesis in *talA*$^-$ cells (see Fig. S1 in the supplemental material), to examine whether the overexpression of talin A-GFP compensates for the loss of talin B. Western blotting analysis confirmed the overexpression of talin A-GFP in the transformant (Fig. 7A). On nonnutrient agar, the talin A-GFP-expressing *talB*$^-$ cells formed mounds, many of which proceeded further to form aberrant fruiting body-like structures (Fig. 7B). The representative terminal structures had a tiny cell mass on top of a stalk extending from a thick column or formed an irregularly shaped bolus on a column (Fig. 7C and D). This result implies that the overexpression of talin A, at least in part, compensates for the loss of talin B during development. Interestingly, we also found that the expression of talin A was upregulated in *talB*$^-$ cells (Fig. 7A), while the expression of talin B was not significantly increased in *talA*$^-$ cells (Fig. 4A).

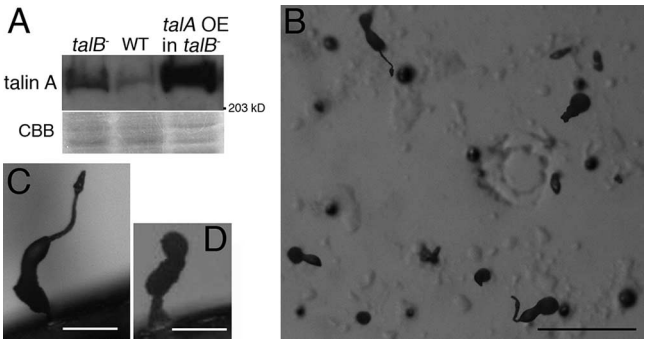


FIG. 7. Developmental defects of a *talB*$^-$ mutant partially rescued by the overexpression of talin A-GFP. (A) Mounds formed by the wild type (WT), the *talB*$^-$ mutant, and the transformant expressing talin A-GFP (*talA* OE in *talB*$^-$) were lysed in SDS sample buffer. Equal amounts of lysates were separated by two individual SDS-PAGEs. One was used for the staining with Coomassie blue (CBB) to show the loading amounts, and the other was used to examine the expression of internal talin A or talin A-GFP by Western blotting analysis using anti-talin A antibody. Overexpression of talin A-GFP in the transformant was confirmed, and the expression of talin A was found to be upregulated in *talB*$^-$ cells. Only a portion of the gel is shown for staining of Coomassie blue. (B) Top view of the final structures of *talA* OE in *talB*$^-$ developed on nonnutrient agar. (C and D) Two representative final structures of *talA* OE in *talB*$^-$ developed on nonnutrient agar. The scale bars represent 1 mm (B), and 40 μm (C and D).

**Movement of *talA*$^-$ *talB*$^-$ cells at the early developmental stage.** Individual *talB*$^-$ cells migrate less effectively than wild-type cells during development, which would explain the developmental block at the tight-mound stage (36). We expected that the mound formation without distinct streams and earlier developmental arrest of *talA*$^-$ *talB*$^-$ mutant might have resulted from more seriously impaired motility in the early stage of development; therefore, we compared the cell locomotion of wild-type, *talA*$^-$, *talB*$^-$, and *talA*$^-$ *talB*$^-$ cells at 4 h after onset of starvation in $KK_2$ phosphate buffer. The starved *talA*$^-$ *talB*$^-$ cells were unable to move on glass surfaces (data not shown). Since we found that placing a thin agar sheet over wild-type cells in this stage enhanced locomotion, we decided to examine the motility of mutant cells in more detail under these agar overlay conditions. Both *talA*$^-$ and *talB*$^-$ cells migrated as actively as wild-type cells under these conditions (Fig.

TABLE 1. Mean motility rates of wild-type and talin mutant strains[a]

| Strain | Velocity (μm/min) | No. of cells measured |
|---|---|---|
| Wild type | 3.88 ± 0.69 | 10 |
| *talA*$^-$ | 3.45 ± 0.89 | 12 |
| *talB*$^-$ | 4.43 ± 1.24 | 11 |
| *talA*$^-$ *talB*$^-$ | ND | |

[a] Mean motility rates of each strain in the condition described in the legend to Fig. 8 are shown as means ± SD. Because *talA*$^-$ and *talB*$^-$ cells did not move, motility rates were not determined (ND).

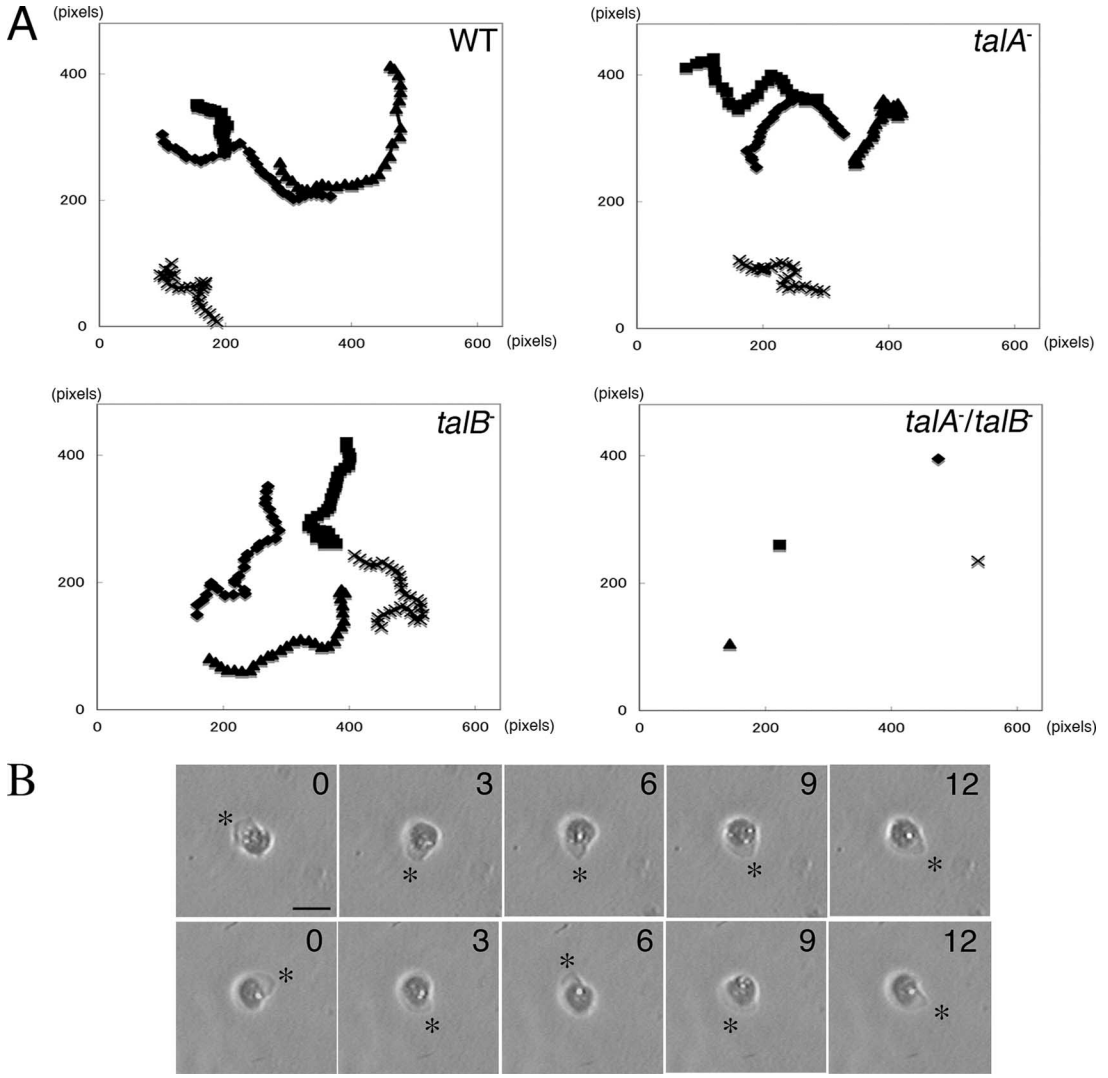


FIG. 8. Random movements in wild-type (WT), *talA*$^-$, *talB*$^-$, and *talA*$^-$ *talB*$^-$ cells starved for 4 h between a glass surface and an overlaid agar sheet. (A) Four representative traces of the random movements of each strain. Cell images were recorded every 3 min for 90 min. 1 pixel corresponds to 1.1 μm. (B) Panels show sequential recordings of two representative *talA*$^-$ *talB*$^-$ cells over a period of 12 min. The cells extended lamellipodia actively (asterisks). Time (in minutes) is indicated at the upper right of each panel. The scale bar represents 20 μm.

8A and Table 1). In contrast, *talA*$^-$ *talB*$^-$ cells extended lamellipodia actively but did not show displacements, even when the motility of wild-type cells was enhanced (Fig. 8A and B).

As *talA*$^-$ *talB*$^-$ cells failed to translocate under the experimental conditions described above, we investigated whether the cells form any adhesive structures. For this purpose, GFP-paxillin and GFP-actin constructs were introduced into wild-type and *talA*$^-$ *talB*$^-$ cells separately, since both molecules are known to accumulate at adhesion sites (2, 5, 38). Confocal microscopic observations identified a dot-like fluorescence of GFP-paxillin on the substrate-attached surfaces in transformants derived from wild-type cells. Dot-like fluorescent signals were not observed in the upper sections above the surface, suggesting that the fluorescent dots corresponded to adhesion sites (Fig. 9A) (see Fig. S2 in the supplemental material). However, the dot-like signals of GFP-paxillin were not observed on the substrate-attached surfaces of the transformants derived from the *talA*$^-$ *talB*$^-$ mutant (Fig. 9B). In contrast, GFP-actin dots were observed on the substrate-attached surfaces of both wild-type and *talA*$^-$ *talB*$^-$ cells (Fig. 9C and D).

## DISCUSSION

The redundant and specific properties of two talins have attracted much interest since second talins were identified recently for various organisms (30). However, only limited information has been obtained regarding this issue. The functions of both talin A and talin B in *Dictyostelium* have been comprehensively investigated by analyses of each single mutant. These studies favored the notions that talin A is important for the vegetative stage, whereas talin B is required for proceeding through development, and that each talin has unique functions (26, 35, 36). These ideas are consistent with the time courses of the expression levels of talin A and talin B. The accumulation

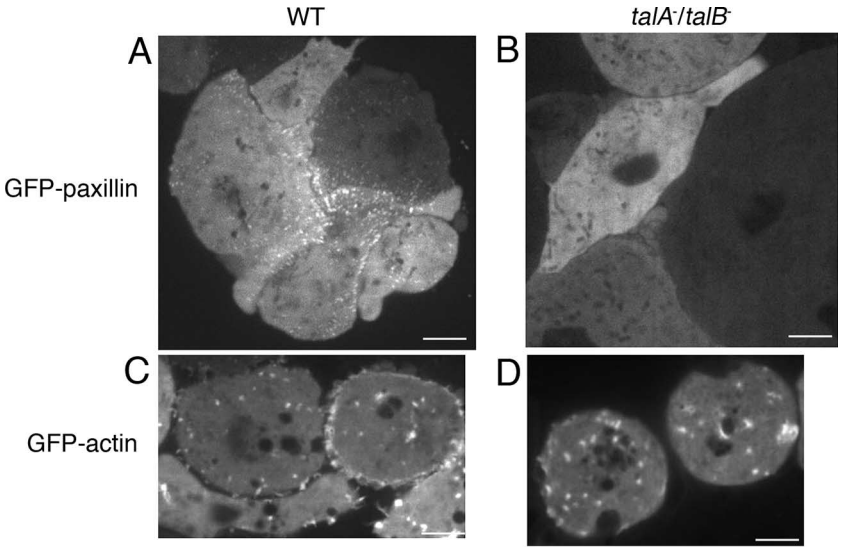


FIG. 9. Adhesion sites in wild-type (WT) and *talA*$^-$ *talB*$^-$ cells visualized by fluorescence microscopy. Fluorescent images of GFP-paxillin (A and B) and GFP-actin (C and D) at the substrate-attached surfaces in the wild-type (A and C) and *talA*$^-$ *talB*$^-$ (B and D) transformants. The fluorescent signals of GFP-paxillin and GFP-actin were observed using confocal microscopy. Adhesion sites revealed by GFP-paxillin were exhibited not only in wild-type cells forming clumps but also in single cells (see Fig. S2 in the supplemental material). The scale bars represent 5 μm.

of talin A was maximal in the vegetative stage, although the transcript of *talA* gene was reported to be constantly expressed (18). In contrast, the accumulation of talin B reached the peak between the mound and slug stages, which roughly correlates with the kinetics of the expression of *talB* mRNA (35). In this study, however, *talA*$^-$ *talB*$^-$ cells exhibited more-severe defects than *talA*$^-$ and *talB*$^-$ cells in adhesion to the substrates and cytokinesis of vegetative cells, and in developmental arrest. These findings indicate that talin A and talin B also work in the developmental and vegetative stages, respectively, despite the fact that each single mutant did not show any detectable alterations in these stages. Furthermore, overexpression of each tagged-talin in the other talin disruptants largely rescued their impaired functions. Hence, this is the first report that demonstrates that two talin homologues in an organism have overlapping functions. We also found that the expression of talin A was upregulated in *talB*$^-$ cells, suggesting that there is cross talk between the two talins. The mechanism of regulation should be addressed in the future.

Although the distinct functions of these two mammalian talins have been emphasized, it is conceivable that they are also able to compensate for the loss of each other. Several cell lines lacking talin 1 do not show serious adhesion defects despite the fact that talin is a major molecule for activating an adhesion receptor, integrin (12, 29). In those cells, talin 2 may mediate the adhesion of cells lacking talin 1, as either talin A or talin B is sufficient for the substrate attachment in *Dictyostelium* vegetative cells. Further research into the elimination or knockdown of both talins in mammalian cells would be required to reveal the full extent of the defects caused by the loss of talin and the complete spectrum of talin's functions.

The stage-specific impairments of *talA*$^-$ and *talB*$^-$ cells could be caused by a reduction of the total amount of talin molecules if the properties of the two talins are completely redundant. In contrast to this model, overexpression of each tagged talin was unable to fully correct the defects of the mutant lacking the other talin, suggesting that talin A and talin B have specific functions. However, we cannot exclude the possibilities that a certain proportion of transformed cells did not express sufficient levels of the tagged talins and that this caused the defects manifested by the population of transformed cells or that the tagged talins were not fully functional for some unknown reasons.

*talA*$^-$ *talB*$^-$ cells completely lost the ability to attach to the substrates in the vegetative stage, suggesting that no other molecule is able to replace talin in this stage. Vertebrate talin generally mediates adhesion by activating integrin (6, 34). Five *Dictyostelium* molecules have been reported to have several features that are common with vertebrate integrin β, which include binding activity to talin (7). We speculate that *Dictyostelium* talin mediates adhesion through these molecules. In contrast to the vegetative stage, *talA*$^-$ *talB*$^-$ cells gained adhesion ability within 5 min when they were transferred to phosphate buffer. Thus, there is another adhesion mechanism, which is blocked in HL5 medium but active in phosphate buffer. Dot-like fluorescence of GFP-actin at the substrate-attached surfaces of *talA*$^-$ *talB*$^-$ cells sandwiched between a glass surface and an agar sheet of phosphate buffer also implies that they are capable of forming adhesion structures in the absence of HL5 medium, although it is not yet proven whether all of the GFP-actin dots are involved in substrate adhesion. Certain mutants generated by chemical mutagenesis were reported to be defective in attachment to a plastic surface in HL5 medium but not in phosphate buffer (37). The study suggested that adhesion molecules were altered in the mutants, though the genes responsible for this defect have not been identified. We suggest that the genes mutagenized in those strains were related to talin functions, though they cannot be talin itself, since a single knockout of one of the two talin genes did not elicit severe defects in substrate adhesion. Further studies need

to be done to characterize the culture medium-sensitive, talin-independent adhesion.

Both talins are also important after starvation in *Dictyostelium*. The adhesion strength of *talA*$^-$ *talB*$^-$ cells was lower than that of wild-type cells even in phosphate buffer, and the cell motility was impaired in the early developmental stage in *talA*$^-$ *talB*$^-$ cells. In addition, talin is required for the formation of adhesion structures containing paxillin. A similar function of talin has been reported for mammalian cells. Although undifferentiated embryonic stem cells from talin 1-deficient mice are able to adhere to fibronectin, the adhesion structures do not contain paxillin. Also, talin 1-deficient mouse fibroblast-like cells are delayed in the initiation of the formation of paxillin-containing focal adhesions (12). Actin-rich dots and paxillin-rich dots were proposed to be distinct structures in *Dictyostelium* because their appearances and dynamics are different (5). Our study also showed that the dimensions of the dots enriched with GFP-paxillin were relatively smaller than the ones enriched with GFP-actin, and the dots of GFP-paxillin were localized in the peripheral region of the substrate-attached surfaces, while the dots of GFP-actin were evenly distributed. *talA*$^-$ *talB*$^-$ cells on nonnutrient agar were able to aggregate and develop until reaching the loose-mound stage. Therefore, they should be able to adhere to and obtain traction forces from the substrates. We speculate that the adhesion system represented by GFP-actin dots enable *talA*$^-$ *talB*$^-$ cells to develop until the loose-mound stage is reached. In addition, cell-cell adhesion might help *talA*$^-$ *talB*$^-$ cells to aggregate, because *talA*$^-$ *talB*$^-$ cells gradually packed into mounds rather than forming streams composed of actively moving cells, which appeared to be mediated by cell-cell adhesion. The paxillin-containing adhesion sites would be important for proper cell adhesions and transmission of motile forces in development.

## ACKNOWLEDGMENTS

We thank Kei Inouye, Department of Botany, Kyoto University, Japan, for his valuable comments on the manuscript.

This study was supported in part by Japan Society for the Promotion of Science and Special Postdoctoral Researchers Program of RIKEN.

## REFERENCES

1. **Albiges-Rizo, C., P. Frachet, and M. R. Block.** 1995. Down regulation of talin alters cell adhesion and the processing of the alpha 5 beta 1 integrin. J. Cell Sci. **108:**3317–3329.
2. **Asano, Y., T. Mizuno, T. Kon, A. Nagasaki, K. Sutoh, and T. Q. Uyeda.** 2004. Keratocyte-like locomotion in amiB-null *Dictyostelium* cells. Cell Motil. Cytoskelet. **59:**17–27.
3. **Bellissent-Waydelich, A., M. T. Vanier, C. Albiges-Rizo, and P. Simon-Assmann.** 1999. Talin concentrates to the midbody region during mammalian cell cytokinesis. J. Histochem. Cytochem. **47:**1357–1368.
4. **Bolton, S. J., S. T. Barry, H. Mosley, B. Patel, B. M. Jockusch, J. M. Wilkinson, and D. R. Critchley.** 1997. Monoclonal antibodies recognizing the N- and C-terminal regions of talin disrupt actin stress fibers when microinjected into human fibroblasts. Cell Motil. Cytoskelet. **36:**363–376.
5. **Bukahrova, T., G. Weijer, L. Bosgraaf, D. Dormann, P. J. van Haastert, and C. J. Weijer.** 2005. Paxillin is required for cell-substrate adhesion, cell sorting and slug migration during *Dictyostelium* development. J. Cell Sci. **118:**4295–4310.
6. **Calderwood, D. A., R. Zent, R. Grant, D. J. Rees, R. O. Hynes, and M. H. Ginsberg.** 1999. The Talin head domain binds to integrin beta subunit cytoplasmic tails and regulates integrin activation. J. Biol. Chem. **274:**28071–28074.
7. **Cornillon, S., L. Gebbie, M. Benghezal, P. Nair, S. Keller, B. Wehrle-Haller, S. J. Charette, F. Bruckert, F. Letourneur, and P. Cosson.** 2006. An adhesion molecule in free-living *Dictyostelium* amoebae with integrin beta features. EMBO Rep. **7:**617–621.
8. **Critchley, D. R.** 2004. Cytoskeletal proteins talin and vinculin in integrin-mediated adhesion. Biochem. Soc. Trans. **32:**831–836.
9. **Di Paolo, G., L. Pellegrini, K. Letinic, G. Cestra, R. Zoncu, S. Voronov, S. Chang, J. Guo, M. R. Wenk, and P. De Camilli.** 2002. Recruitment and regulation of phosphatidylinositol phosphate kinase type 1 gamma by the FERM domain of talin. Nature **420:**85–89.
10. **Early, A. E., and J. G. Williams.** 1989. Identification of sequences regulating the transcription of a *Dictyostelium* gene selectively expressed in prespore cells. Nucleic Acids Res. **17:**6473–6484.
11. **Eichinger, L., J. A. Pachebat, G. Glockner, M. A. Rajandream, R. Sucgang, M. Berriman, J. Song, R. Olsen, K. Szafranski, Q. Xu, B. Tunggal, S. Kummerfeld, M. Madera, B. A. Konfortov, F. Rivero, A. T. Bankier, R. Lehmann, N. Hamlin, R. Davies, P. Gaudet, P. Fey, K. Pilcher, G. Chen, D. Saunders, E. Sodergren, P. Davis, A. Kerhornou, X. Nie, N. Hall, C. Anjard, L. Hemphill, N. Bason, P. Farbrother, B. Desany, E. Just, T. Morio, R. Rost, C. Churcher, J. Cooper, S. Haydock, N. van Driessche, A. Cronin, I. Goodhead, D. Muzny, T. Mourier, A. Pain, M. Lu, D. Harper, R. Lindsay, H. Hauser, K. James, M. Quiles, M. Madan Babu, T. Saito, C. Buchrieser, A. Wardroper, M. Felder, M. Thangavelu, D. Johnson, A. Knights, H. Loulseged, K. Mungall, K. Oliver, C. Price, M. A. Quail, H. Urushihara, J. Hernandez, E. Rabbinowitsch, D. Steffen, M. Sanders, J. Ma, Y. Kohara, S. Sharp, M. Simmonds, S. Spiegler, A. Tivey, S. Sugano, B. White, D. Walker, J. Woodward, T. Winckler, Y. Tanaka, G. Shaulsky, M. Schleicher, G. Weinstock, A. Rosenthal, E. C. Cox, R. L. Chisholm, R. Gibbs, W. F. Loomis, M. Platzer, R. R. Kay, J. Williams, P. H. Dear, A. A. Noegel, B. Barrell, and A. Kuspa.** 2005. The genome of the social amoeba *Dictyostelium discoideum*. Nature **435:**43–57.
12. **Giannone, G., G. Jiang, D. H. Sutton, D. R. Critchley, and M. P. Sheetz.** 2003. Talin1 is critical for force-dependent reinforcement of initial integrin-cytoskeleton bonds but not tyrosine kinase activation. J. Cell Biol. **163:**409–419.
13. **Goldmann, W. H., D. Hess, and G. Isenberg.** 1999. The effect of intact talin and talin tail fragment on actin filament dynamics and structure depends on pH and ionic strength. Eur. J. Biochem. **260:**439–445.
14. **Hibi, M., A. Nagasaki, M. Takahashi, A. Yamagishi, and T. Q. Uyeda.** 2004. *Dictyostelium discoideum* talin A is crucial for myosin II-independent and adhesion-dependent cytokinesis. J. Muscle Res. Cell Motil. **25:**127–140.
15. **Jermyn, K. A., K. T. Duffy, and J. G. Williams.** 1989. A new anatomy of the prestalk zone in *Dictyostelium*. Nature **340:**144–146.
16. **Jiang, G., G. Giannone, D. R. Critchley, E. Fukumoto, and M. P. Sheetz.** 2003. Two-piconewton slip bond between fibronectin and the cytoskeleton depends on talin. Nature **424:**334–337.
17. **Joly, E., D. Traynor, K. Jermyn, and J. Kirk.** 1993. Addition of heat-killed bacteria to the selective medium enhances transformation of *Dictyostelium discoideum*. Trends Genet. **9:**157–158.
18. **Kreitmeier, M., G. Gerisch, C. Heizer, and A. Muller-Taubenberger.** 1995. A talin homologue of *Dictyostelium* rapidly assembles at the leading edge of cells in response to chemoattractant. J. Cell Biol. **129:**179–188.
19. **Lee, S. Y., S. Voronov, K. Letinic, A. C. Nairn, G. Di Paolo, and P. De Camilli.** 2005. Regulation of the interaction between PIPKI gamma and talin by proline-directed protein kinases. J. Cell Biol. **168:**789–799.
20. **Levi, S., M. Polyakov, and T. T. Egelhoff.** 2000. Green fluorescent protein and epitope tag fusion vectors for *Dictyostelium discoideum*. Plasmid **44:**231–238.
21. **Ling, K., R. L. Doughman, A. J. Firestone, M. W. Bunce, and R. A. Anderson.** 2002. Type I gamma phosphatidylinositol phosphate kinase targets and regulates focal adhesions. Nature **420:**89–93.
22. **McCann, R. O., and S. W. Craig.** 1999. Functional genomic analysis reveals the utility of the I/LWEQ module as a predictor of protein:actin interaction. Biochem. Biophys. Res. Commun. **266:**135–140.
23. **Monkley, S. J., X. H. Zhou, S. J. Kinston, S. M. Giblett, L. Hemmings, H. Priddle, J. E. Brown, C. A. Pritchard, D. R. Critchley, and R. Fassler.** 2000. Disruption of the talin gene arrests mouse development at the gastrulation stage. Dev. Dyn. **219:**560–574.
24. **Morgan, J. R., G. Di Paolo, H. Werner, V. A. Shchedrina, M. Pypaert, V. A. Pieribone, and P. De Camilli.** 2004. A role for talin in presynaptic function. J. Cell Biol. **167:**43–50.
25. **Nagasaki, A., E. L. de Hostos, and T. Q. Uyeda.** 2002. Genetic and morphological evidence for two parallel pathways of cell-cycle-coupled cytokinesis in *Dictyostelium*. J. Cell Sci. **115:**2241–2251.
26. **Niewohner, J., I. Weber, M. Maniak, A. Muller-Taubenberger, and G. Gerisch.** 1997. Talin-null cells of *Dictyostelium* are strongly defective in adhesion to particle and substrate surfaces and slightly impaired in cytokinesis. J. Cell Biol. **138:**349–361.
27. **Nuckolls, G. H., L. H. Romer, and K. Burridge.** 1992. Microinjection of antibodies against talin inhibits the spreading and migration of fibroblasts. J. Cell Sci. **102:**753–762.
28. **Powell-Coffman, J. A., G. R. Schnitzler, and R. A. Firtel.** 1994. A GBF-binding site and a novel AT element define the minimal sequences sufficient to direct prespore-specific expression in *Dictyostelium discoideum*. Mol. Cell. Biol. **14:**5840–5849.
29. **Priddle, H., L. Hemmings, S. Monkley, A. Woods, B. Patel, D. Sutton, G. A. Dunn, D. Zicha, and D. R. Critchley.** 1998. Disruption of the talin gene

compromises focal adhesion assembly in undifferentiated but not differentiated embryonic stem cells. J. Cell Biol. **142:**1121–1133.
30. **Senetar, M. A., and R. O. McCann.** 2005. Gene duplication and functional divergence during evolution of the cytoskeletal linker protein talin. Gene **362:**141–152.
31. **Senetar, M. A., C. L. Moncman, and R. O. McCann.** 2007. Talin2 is induced during striated muscle differentiation and is targeted to stable adhesion complexes in mature muscle. Cell Motil. Cytoskelet. **64:**157–173.
32. **Singiser, R. H., and R. O. McCann.** 2006. Evidence that talin alternative splice variants from *Ciona intestinalis* have different roles in cell adhesion. BMC Cell Biol. **7:**40.
33. **Sussman, M.** 1987. Cultivation and synchronous morphogenesis of *Dictyostelium* under controlled experimental conditions. Methods Cell Biol. **28:**9–29.
34. **Tadokoro, S., S. J. Shattil, K. Eto, V. Tai, R. C. Liddington, J. M. de Pereda, M. H. Ginsberg, and D. A. Calderwood.** 2003. Talin binding to integrin beta tails: a final common step in integrin activation. Science **302:**103–106.
35. **Tsujioka, M., L. M. Machesky, S. L. Cole, K. Yahata, and K. Inouye.** 1999. A unique talin homologue with a villin headpiece-like domain is required for multicellular morphogenesis in *Dictyostelium*. Curr. Biol. **9:**389–392.
36. **Tsujioka, M., K. Yoshida, and K. Inouye.** 2004. Talin B is required for force transmission in morphogenesis of *Dictyostelium*. EMBO J. **23:**2216–2225.
37. **Vogel, G., L. Thilo, H. Schwarz, and R. Steinhart.** 1980. Mechanism of phagocytosis in *Dictyostelium discoideum*: phagocytosis is mediated by different recognition sites as disclosed by mutants with altered phagocytotic properties. J. Cell Biol. **86:**456–465.
38. **Yumura, S., and T. Kitanishi-Yumura.** 1990. Fluorescence-mediated visualization of actin and myosin filaments in the contractile membrane-cytoskeleton complex of *Dictyostelium discoideum*. Cell Struct. Funct. **15:**355–364.